Electroplating of CdTe thin films from cadmium sulphate precursor and comparison of layers grown by 3-electrode and 2-electrode systems

DHARMADASA, I <http://orcid.org/0000-0001-7988-669X>, MADUGU, Mohammad L., OLUSOLA, Olajide I., ECHENDU, Obi K, FAUZI, Fijay, DISO, Dahiru, WEERADINGHE, Ajith, DHARMADASA, Ruvini, LAVERY, Brandon, JASINSKI, Jacek B., KRENTSEL, Tatiana A. and SUMANASEKERA, Gamini

coatings

MDPI

Article

Electroplating of CdTe Thin Films from Cadmium Sulphate Precursor and Comparison of layers grown by 3-electrode and 2-electrode systems

Imyhamy M. Dharmadasa, Mohammad L. Madugu *, Olajide I. Olusola, Obi K. Echendu [1], Fijay Fauzi [2], Dahiru G. Diso [3], Ajith R. Weerasinghe [4], Thad Druffel [5], Ruvini Dharmadasa [5], Brandon Lavery [5] Jacek B. Jasinski [5], Tatiana A. Krentsel [5], and Gamini Sumanasekera [5]

Keywords: Electrodeposition; CdTe; $CdSO_4$ precursor; solar energy materials; CdS/CdTe solar cells

1. Introduction

Cadmium telluride (CdTe) thin films have received much attention due to their various applications in electronic devices such as solar cells [1] and X- and γ-radiation detectors [2]. The increase in demand for clean and sustainable energy is a huge challenge for the photovoltaic (PV) community to develop low-cost and high efficiency solar panels. The present sources of energy which are mostly from fossil fuel are harmful to the sustainability of our ecosystem. Alternative technologies such as the photovoltaics (PV) which convert sunlight in to clean energy have been the main research focus at present [3]. The II-VI semiconductor materials have been found suitable in complementing this effort. Among these semiconductors, CdTe stands out to be one of the most researched and promising semiconductor materials in the production of both laboratory scale and large area optoelectronic devices such as the solar panels. CdTe has a direct and near ideal bandgap of 1.45 eV for one bandgap and single p-n junction solar cells with high absorption coefficient (>10^4 cm^{-1}) [4]. CdTe can be n- or p-type in electrical conduction [5,6] depending on the stoichiometry or intentionally added dopants. These are among the properties that make it a suitable material for application in solar energy conversion. CdTe can be grown using low-cost techniques and the material can absorb over 90% of photons with energy greater than E_g=1.45 eV using only about 2.0 μm thick layer.

CdTe thin films have been grown using a large number of deposition techniques [7]. Some of the main techniques used are close-spaced sublimation (CSS) [2], sintering [8], electrodeposition (ED) [1], molecular beam epitaxy (MBE) [9], metalorganic chemical vapour deposition (MOCVD) [10], pulsed laser deposition (PLD) [11], etc. Electrodeposition is a simple and low-cost technique, and offers an advantage of growing materials with both n-type and p-type electrical conductivity by simply changing the growth potential using single electrolytic bath and it produces electronic device quality films for solar cell fabrication.

In electrodeposition, CdTe can be cathodically synthesised using either aqueous [1,12] or non-aqueous [13] electrolytes in acidic (pH=1.00-3.00) or alkaline medium (pH=8.40-10.70 [14,15]. The choice of acidic rather than alkaline medium for the electrodeposition of CdTe is due to the fact that Te is more soluble and stable in acidic medium. The history of CdTe growth based on electrodeposition using aqueous electrolyte was first demonstrated by Mathers and Turner in 1928 [13]. A more elaborate work on the electrodeposition of CdTe was carried out by Panicker and Knaster in 1978 [12], and thereafter many researchers [1,15-19] have electrodeposited CdTe from aqueous solutions. Usually, the electrodeposition of CdTe is carried out using $CdSO_4$ and TeO_2 which serves as Cd and Te precursors respectively. Research programme continued by BP in the 1980s successfully demonstrated the scaling up of this technology by manufacturing nearly 1.0 m^2

area solar panels with over 10% conversion efficiency [18]. The successful deposition of CdTe and comprehensive material characterisation have also been carried out recently using $CdCl_2$ [14] and $Cd(NO_3)_2$ precursors [19] for selecting the best cadmium precursor for electroplating. The recent announcement of 22.1% efficiency of CdTe solar cells by First Solar company [20] using CdTe grown by vapour transport deposition (VTD), is a giant stride in the PV field showing great potential in CdTe based thin film solar cells. With all these attractive properties, CdS/CdTe solar cell efficiency improvement was mostly hindered for decades by a number of challenges; limited know-how on material issues, processing steps and device physics has been the major bottle-necks. Achieving large grains, uniform, dense and pinholes free thin films with minimum defects and optimum doping concentration have been identified as one of the challenges faced by the PV community.

During the past three decades, CdS/CdTe solar cell research was carried out assuming CdTe layer in the device as a p-type material. Therefore, all experimental results were interpreted based on a simple p-n junction model. This has led to stagnation of the development of this device for a long period of time. The results presented in this paper aims to demonstrate that both p-type and n-type CdTe layers can be grown easily by changing its composition. Furthermore, this work aims to show that layers may remain n-type after post-growth heat treatments. Therefore, the new work aims to demonstrate that p-n junction devices and other complex n-n-n-Schottky Barrier type devices are possible from this material and the latter seems more efficient in solar energy conversion.

The paper also compares the results obtained from CdTe layers grown by 3-electrode (3E) and 2-electrode (2E) configuration, in order to gauge the best approach for minimisation of impurities. Ag^+ ions and other group-I ions such as Na^+ and K^+ are highly poisonous to CdTe solar cells [21] and the removal of reference electrode from the electrolyte could be highly beneficial for achieving high performance devices. Reference electrodes usually have a saturated KCl solution outer jacket in commercially available products with a possibility of leaking K^+ into the electrolyte. The preliminary studies on the comparison of 3E and 2E systems were published recently by Echendu *et al* [22]. This paper present the results of a comprehensive study in order to confirm the conclusions arrived at initial stages. Removal of the reference electrode from the electrodeposition system introduces several advantages in order to reduce the cost of CdS/CdTe solar cells further. Elimination of a possible impurity source and hence achieving high conversion efficiencies, system simplification, cost reduction and ability to grow improved materials at temperatures higher than the reference electrode limit (70^oC) are some of the advantages.

In this paper, we present the summary of results for CdTe thin films grown from aqueous and acidic electrolyte containing $CdSO_4$ and TeO_2 using potentiostatic cathodic electrodeposition. After deposition, the films were characterised using a wide range of analytical techniques for structural, morphological, optical and electrical properties. This paper presents the comparison of CdTe layers grown by 3E and 2E systems, and their effects on fully fabricated devices. The paper also provides the new insight into physics of new devices based on CdTe thin films.

2. Experimental details

2.1 Chemicals and materials used

In this work, cadmium sulphate ($CdSO_4$) powder with purity ≥99% was used as the source of Cd while the source of tellurium (Te) was tellurium oxide (TeO_2) powder of high purity (99.999%). The substrate used were fluorine-doped tin oxide (FTO) coated glasses with sheet resistance 13 Ω/square. Dilute sulphuric acid (H_2SO_4) and ammonium hydroxide (NH_4OH) were used for pH adjustment in solutions. All chemicals and substrates were purchased from Sigma-Aldrich UK. The solvent used for the electrolyte preparation was de-ionised water. For the 3E system, a saturated calomel electrode (SCE) was used as the reference with a platinum (Pt) anode. The saturated KCl solution in the outer jacket was replaced by a $Cd(SO_4)$ solution in order to avoid K leakage into the electrolyte. Carbon (C) rod was used as the anode for the 2E system. A clean glass/FTO substrate was used as the cathode for both systems. The source of power was a computerised Gill AC potentiostat and the heating of the bath was provided by hot-plate with magnetic stirrer.

The containers used were Teflon beakers of 1000 ml for the electrolyte and 2000 ml pyrex beakers of 2000 ml for the outer jacket. Polytetrafluoroethylene (PTFE) tape was used to hold the glass/FTO substrates to the carbon connecting rod during deposition. The cleaning of the substrates was carried out using organic solvents (methanol & acetone) and de-ionised water.

2.2 Preparation of Electrolytic Cells

The electrolytic baths were prepared from aqueous solutions of 1M $CdSO_4$ and TeO_2 solution in 800 ml of deionised water contained in a 1000 ml Teflon beaker. The solution containing only low purity $CdSO_4$ was electropurified for ~50 hours before adding the high purity TeO_2 dilute solution. The main reason for using low-purity $CdSO_4$ is the requirement of large amount of $CdSO_4$ for this work and very high cost of the high-purity $CdSO_4$. The TeO_2 was separately prepared by dissolving TeO_2 powder using dilute sulphuric acid for addition to the electrolyte. The pH of the bath was adjusted to 2.00±0.02 using H_2SO_4 acid or NH_4OH prior to CdTe deposition.

The choice of materials to be employed for this experiment is important since the medium of growth is acidic (pH=2.00). The acidic electrolyte has been shown to absorb impurities from glass containers and the carbon anode in direct contact. This contamination can be minimised by reducing the contacts between the electrolyte and glass surfaces. [13]. Therefore, the Teflon beakers were used as the electrolyte containing vessels for both 3E and 2E systems. This is to minimise impurities which affects final device parameters when incorporated into the CdTe layer during growth.

2.3. Analytical Techniques used.

A wide range of analytical techniques were used to investigate the electroplated CdTe layers. To study the structural properties, Philips PW 3710 X' pert pro diffractometer using Cu-K_α excitation wavelength (λ=1.542 Å) was employed and the scan ranges between $2\theta=(20\text{-}60)^o$. The morphology of the film surfaces and grain sizes were observed using FEG NOVA NANO scanning electron microscope (SEM). The study of the molecular vibration to obtain unique finger prints of the materials was carried out using a Renishaw Raman microscope with a CCD detector and 514 nm argon ion laser. The electrical conduction type of the films was detected using a photoelectrochemical (PEC) cell measurement system using an aqueous electrolyte of 0.1M $Na_2S_2O_3$. Optical energy bandgaps were measured using a Cary 50 scan UV-Vis spectrophotometer (Varian Australia Pty. Ltd). The DC electrical conductivity measurements were carried out using a fully automated I-V system including a Keithley 619 electrometer and multimeter (Keithley, Cleveland, OH, USA). Photoluminescence (PL) measurements to observe the defect levels in the bandgap was carried out using Renishaw inVia Raman microscope (Renishaw, Hoffman Estates, IL, USA) with a CCD detector and a 632 nm He-Ne laser excitation source. Intense pulsed light (IPL) heat treatment was carried out in air using Sintering 2000 (Xenon Corporation).

3. Experimental Results

3.1. Cyclic voltammetry

Figure 1 shows typical voltammograms or current-voltage curves of the electrolytes with 3E and 2E electrode systems. Due to the voltage measurement with respect to the reference electrode in 3E and the carbon anode in 2E system, the magnitudes of the cathodic voltages are different in the graphs. Otherwise main features are similar in both cases.

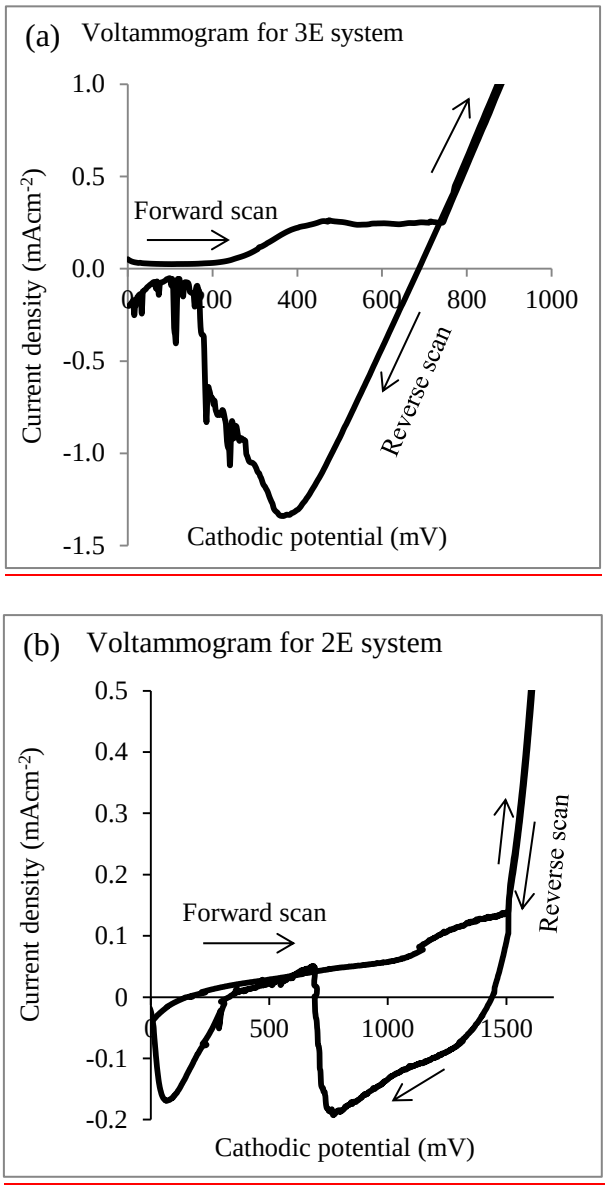

Figure 1. Cyclic voltammograms of aqueous solutions consisting of 1M $CdSO_4$ and low level of TeO_2 with glass/FTO cathode in (a) 3E and (b) 2E systems. The reference electrode used for 3E system is standard calomel electrode. The growth temperature was ~70°C and ~85°C for 3E and 2E systems respectively. The pH of both electrolytes was set to 2.00±0.02 at the beginning of the experiment at room temperature.

The mechanism for the deposition of CdTe on the cathode from acidic aqueous electrolyte as proposed by Panicker et al [12] was given below using equations (1) and (2). The first process which is a diffusion control is the reduction of $HTeO_2^+$ to Te which reacts with Cd^{2+} to form CdTe on the cathode. The formation of CdTe thin films on the cathode is highly influenced by diffusion process. The overall equations for the formation of CdTe on the cathode are given below;

$$HTeO_2^+ + 3H^+ + 4e^- \longrightarrow Te + 2H_2O \quad (1)$$

$$Cd^{2+} + Te + 2e \longrightarrow CdTe \quad (2)$$

Since the redox potential of Te is +0.593 V with respect to standard H_2 electrode, this element is easier to deposit on the cathode first. In the 3E system, Te deposition starts around 200 mV, and then at higher cathodic voltages of around 550 mV Cd starts to deposit (redox potential of Cd is -0.403 V with respect to standard H_2 electrode). As a result when cathodic potential is gradually increased, the sequence of deposition is; Te layer first, Te-rich CdTe second, stoichiometric CdTe third and finally Cd-rich CdTe layers. This transition takes place gradually, and at a certain voltage, stoichiometric CdTe layer is formed. This voltage is labelled as perfect potential of stoichiometry (PPS) in this paper. This is the voltage we expect to find for growing device quality CdTe layers. In the reverse scan, when the cathodic voltage is gradually reduced, material starts to dissolve into the solution. The dissolution order will be elemental Cd first, Cd from CdTe second and finally Te from the cathode surface. This dissolution process creates a current flow in the negative direction. The large peak in the negative current represents the dissolution of both Cd and Te from the cathode surface.

The main features of the voltammogram for 2E system are the same, but the absolute values of the cathodic voltages are different. It should be noted that these deposition voltages are very different from the redox potentials given above. The reason is that the redox potentials are given w.r. to standard H_2 electrode and the measured values in these experiments are w.r. to carbon anode, for 2E and standard calomel electrode for 3E system. Te deposition starts around 250 mV and Cd deposition takes place around 1000 mV. In the reverse direction Cd dissolution and Te dissolution are shown in two separate current peaks. This peak separation can be due to different experimental conditions such as scan rate, different temperature and the stirring rates.

3.2. X-ray diffraction

Careful observation of the voltammogram helps in estimating suitable cathodic voltages for growing stoichiometric CdTe. By growing layers at fixed voltages in this estimated region, and observations using XRD, PEC and optical absorption methods, this estimated voltage range can be reduced to a very narrow range. In this study, these voltages were changed by 2 mV and 1 mV steps for 3E and 2E systems respectively in order to pin-point the perfect potential of stoichiometry (PPS).

Figure 2 shows the XRD spectra measured for samples grown in the vicinity of PPS from both 3E and 2E systems. Figure 2(a) shows the variation of XRD observed for CdTe grown by 3E system. Every effort was taken to grow approximately equal thicknesses and the variation of the intensity of the most intense (111) peak was closely monitored. It was found that the highest intensity was observed when the layers were grown at 834 mV. When heat treated in the presence of $CdCl_2$, the intensity variation remained the same, confirming that the highest crystallinity shifted to 830 mV w.r.t. calomel reference and Pt anode. Therefore, the PPS value for 3E system is confirmed as 830 mV with respect to SCE under the experimental condition used in this work. This voltage was taken as the PPS, since $CdCl_2$ treatment is used prior to fabrication of CdS/CdTe solar cells.

Figure 2(b) and 2(d) show similar results for CdTe grown by 2E system. XRD features remain the same, and PPS for this experimental system can be determined as 1576 mV with respect to the carbon anode. All other XRD features are very similar, but the growth rate is usually faster in 2E system, when compared to the 3E system. This can be taken as an advantage in manufacturing process reducing growth time. In the case of heat treated samples in the presence of $CdCl_2$, the (220) and (311) peaks starts to appear. This shows that the grains are losing their preferential orientation along (111).

In both cases, the (111) peak of as-deposited CdTe layers were used to estimate the crystallite sizes. The use of Scherrer's equation yield (20-65) nm for the crystallite size for both material layers.

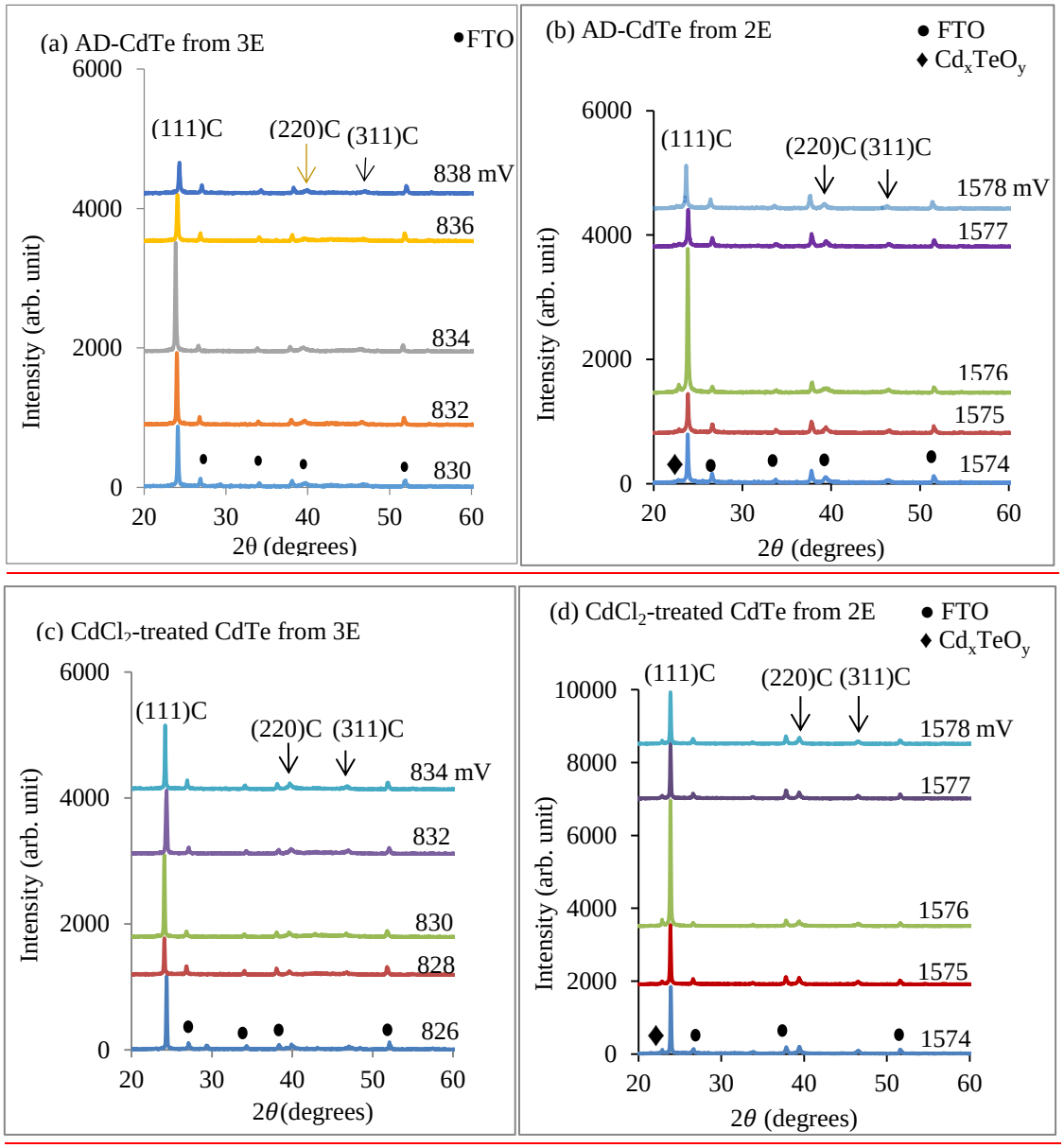

Figure 2. XRD patterns for as-deposited (AD) CdTe films deposited at different growth voltages using 3E (a) and 2E (b) systems. (c) and (d) show XRD patterns for $CdCl_2$-treated layers. All heat-treatments were carried out at 400°C for 15 minutes in air in the presence of $CdCl_2$.

3.3. Scanning electron microscopy

Scanning electron microscopy (SEM) studies were carried out in order to investigate the surface morphology of electroplated CdTe layers using both 3E and 2E systems. Typical results are shown in Figure 3 for both as-deposited and $CdCl_2$ treated layers. The as-deposited layers of 3E (Figure 3a) and 2E (Figure 3b) are covered with large clusters or agglomerations consisting of nano-crystallytes. The clusters have varying sizes up to sub-micron level for largest ones. The small grains are crystalline CdTe and their size varies from (20-65) nm as determined by XRD measurements and Scherrer's equation. There is no noticeable difference in the morphology and crystallite sizes for 3E and 2E grown CdTe layers. Only the cluster size is larger in layers grown by the 2E system.

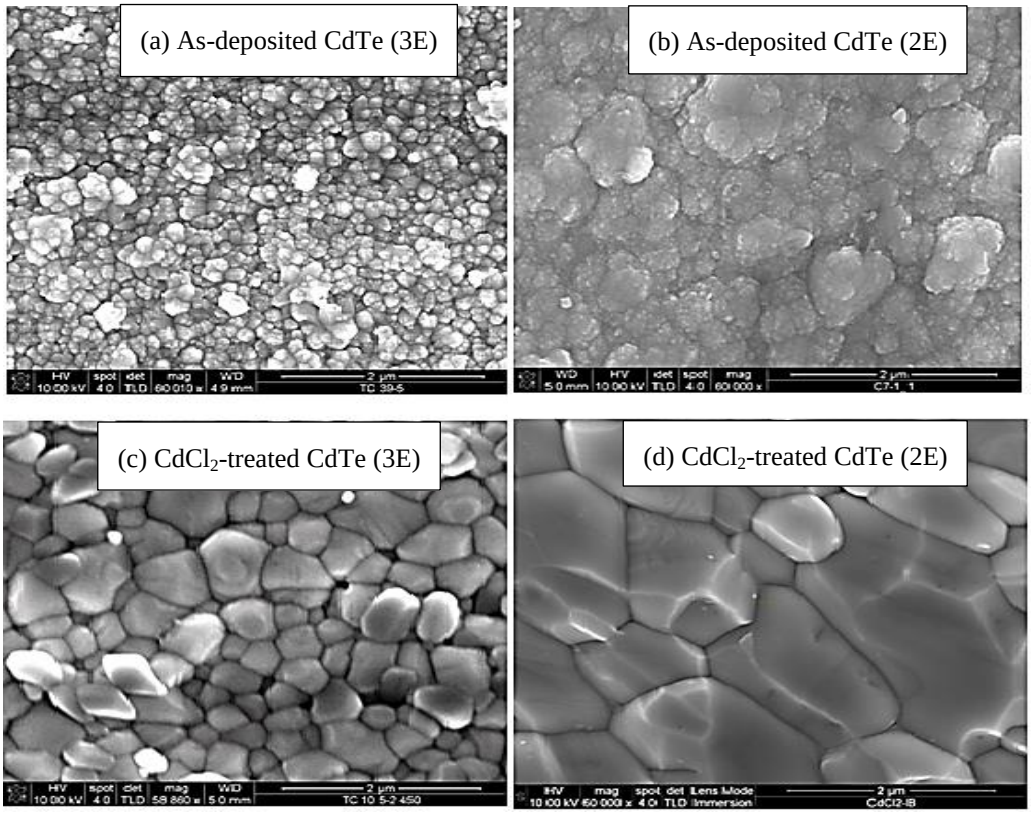

Figure 3. Typical SEM images for as-deposited and $CdCl_2$-treated CdTe layers grown by 3E system (a and c) and 2E system (b and d). $CdCl_2$ treatment was carried out in a conventional furnace at 450°C for 20 minutes in air, in the presence of $CdCl_2$.

Heat treatment at 450°C for 20 minutes in air, in the presence of $CdCl_2$ shows a dramatic change. Nano-crystallites within clusters have merged together to form large crystals, and the clusters become large grains of CdTe. This is thermodynamically expected since the surface to volume ratio is large for nano crystallites. Grain sizes vary in the few microns size and these layers show similarity in structure to CdTe grown by high temperature techniques such close spaced sublimation (CSS).

Prolong heating at temperatures ~450°C makes these grains larger due to Oswald ripening, but detrimental for device performance. This is due to the columnar growth producing larger grains exposing wider gaps between grains. In addition, the material losses due to sublimation have also been observed. Both these processes increase pin-holes or gaps formation and therefore detrimental for final device performance.

The heat treatment is crucial in device performance and the PV solar cell developers are moving towards roll-to-roll production methods. Therefore, Intense Pulse Light (IPL) annealing was also used to study the morphology changes during heat treatment. IPL is a rapid thermal annealing method applicable to materials grown on flexible substrates, and CdTe layer can be heat treated from the top surface using pulses of white light. Heat energy released to the material layer can be controlled by the energy of a pulse and the number of pulses used to heat the layer. Full details of this technique is given in reference [23], and here the main morphology changes of the surfaces are presented and discussed.

Figure 4(a) shows another SEM image of a CdTe layer grown by the 2E system. These surfaces are very similar to the ones shown in Figure 3(a) and 3(b). Small crystallites are clustered together to form large agglomerations. Figures 4(b), 4(c) and 4(d) show the surface morphology after IPL treatments with energy 1730 Jcm^{-2} (100 pulses x 17.3 Jcm^{-2}), 2160 Jcm^{-2} (100 pulses x 21.6 Jcm^{-2}) and 2588 Jcm^{-2} (100 pulses x 25.9 Jcm^{-2}) respectively.

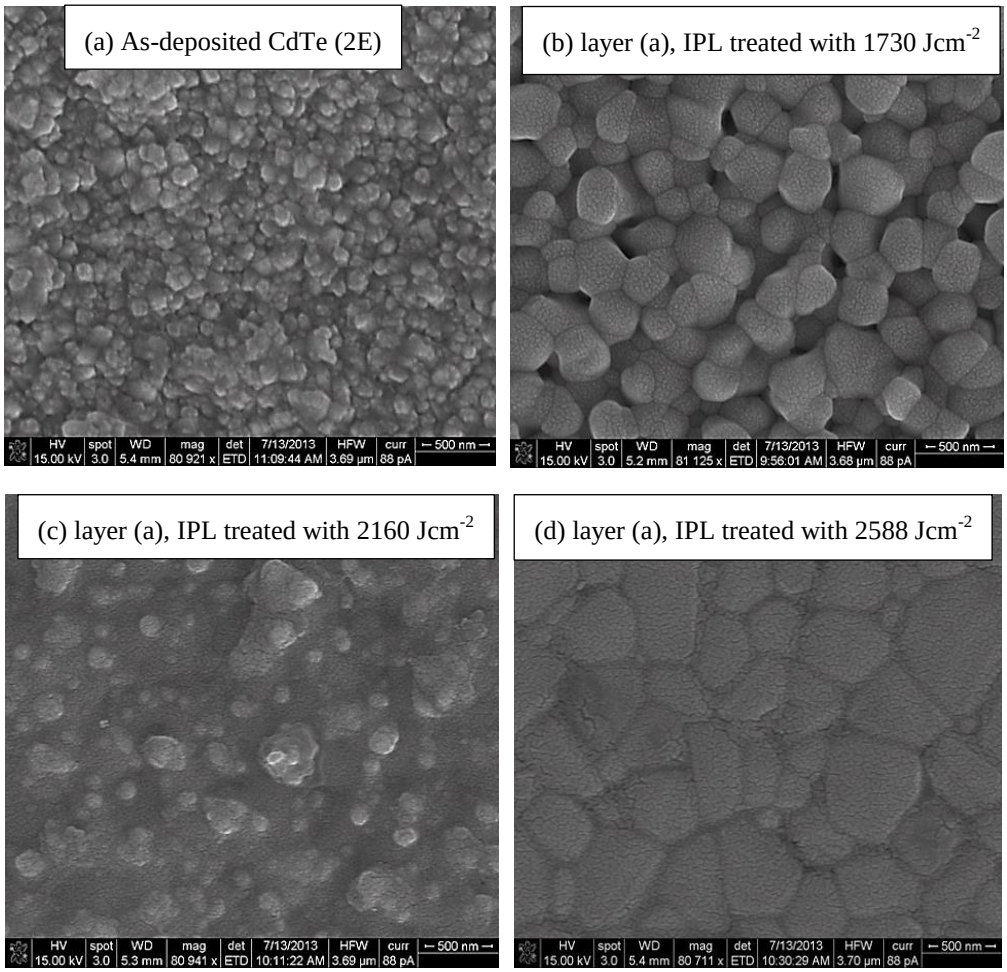

Figure 4. A typical SEM image of as-deposited CdTe layer from 2E system and changes of morphology as the energy input is increased using IPL treatment.

From these SEM images, it is clear that the agglomerations become large crystalline grains, after melting mainly the grain boundary areas and subsequently freezing during cooling. Figure 4(d) clearly shows the large CdTe grains formed across the thin layer. Cross-section SEM images show that those grains have columnar nature, spreading from bottom to top of the thin films. It also shows the melted grain boundaries frozen after heat treatment. As shown by the phase diagram of CdTe [7], the melting point of grain boundary materials with impurities such as O, Cl and excess Cd from $CdCl_2$ are much lower (~350-450°C) than the melting point of pure CdTe grains (1093°C). Therefore during heat treatment, grain boundaries become a liquid allowing CdTe grains to flow, coalesce and grow into large grains.

3.4. Photoelectrochemical cell measurements

In order to use a material in any electronic device and interpret experimental results, its electrical conductivity type must be accurately known. The most accurate method to find this is the conventional Hall Effect measurements, but these studies cannot be performed on glass/FTO/CdTe layers due to the underlying conducting layer of FTO. Electrons find the lowest resistive path and therefore measurements are not at all reliable. For this reason, the Photoelectrochemical (PEC) cell measurements have been used to find the electrical conduction type of these layers.

For these measurements, glass/FTO/CdTe were immersed in any suitable electrolyte (aqueous solution of $Na_2S_2O_3$ for example) in order to form a solid/liquid junction at CdTe/electrolyte interface. This is equivalent to a weak Schottky diode and its open circuit voltage is measured by

measuring its voltage with respect to a counter electrode (graphite rod) immersed in the same electrolyte. The difference between the voltages measured under dark and illuminated conditions provides the PEC signal. After calibrating the system with a known material, the sign of the open circuit voltage or the PEC signal determines the electrical conductivity type of the CdTe layer. The magnitude of the PEC signal indicates the strength of the depletion region formed at the solid/liquid junction, and hence an indirect and qualitative idea of the doping level of CdTe layer. Both insulating and metallic layers provide a zero PEC signal due to non-formation of a healthy depletion region. In our calibrated system, positive PEC signal indicates a p-type semiconductor and a negative signal shows an n-type semiconductor.

Figure 5(a) and (b) show the PEC signals observed for as-deposited and $CdCl_2$ treated CdTe layers grown from both 3E and 2E systems, as a function of growth voltage. Both CdTe materials grown using 3E and 2E systems show similar behaviour. At low cathodic voltages, Te-rich, p-type CdTe layers are grown while at larger cathodic voltages, Cd-rich, n-type CdTe layers are grown. In between these two regions, there exists an inversion voltage (V_i) or perfect potential of stoichiometry (PPS), which produces stoichiometric CdTe with highest crystallinity due to existence of only one phase. Crystallinity of the layers reduces, when grown away from V_i or PPS due to presence of two phases within the layer. The absolute value of V_i vary depending on factors such Te concentration, stirring rate and pH value.

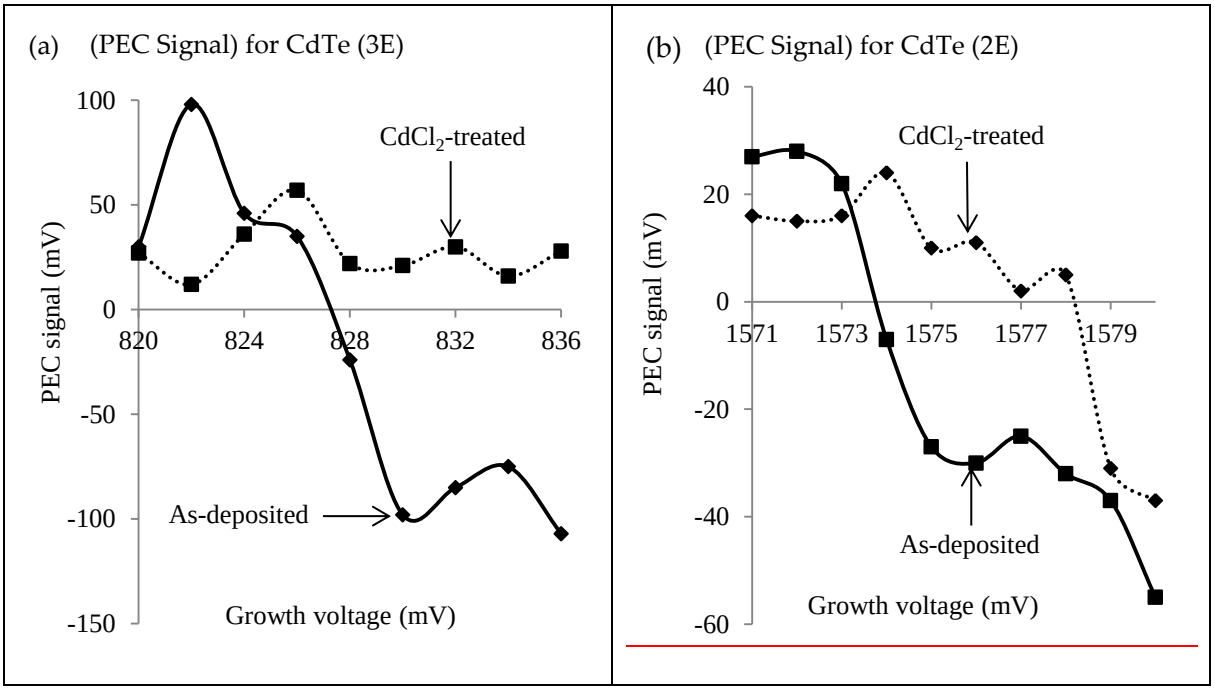

Figure 5. PEC cell measurements for as-grown and $CdCl_2$-treated CdTe thin films deposited using (a) 3E and (b) 2E systems at different growth voltages. Samples were heat-treated at 400℃ for 15 minutes in air in the presence of $CdCl_2$.

Upon $CdCl_2$ treatment, both materials keep the similar behaviour. The p-type nature reduces and moves towards n-type property, and n-type nature reduces and move towards p-type property. It should be noted that this is due to the movement of the Fermi level within the bandgap and complete type conversion may not occur. This shows the direction of movement of the FL in the bandgap depending on initial condition of the layer, doping effects, and annealing out defects during the heat-treatment. These measurements indicate only the electrical conductivity type of the top layers of CdTe materials, since the depletion region formed at the solid/liquid junction is limited only to the surface region.

3.5. Raman studies

Raman scattering studies were carried out in order to use as a non-destructive and quick quality control method. This could be useful in a production line to check the quality of materials grown before processing devices. In our previous Raman studies [14,24,25], peak arising from both CdTe and elemental Te was observed. The X- and γ-ray detectors research community has carried out comprehensive studies on Te-precipitation during CdTe growth [26,27]. In agreement with the reports, we also observe Raman peaks arising from elemental Te in electrodeposited CdTe layers.

Figure 6 shows typical Raman spectra of CdTe layers grown near the PPS, using both 3E (V_g = 828 mV) and 2E (V_g = 1360 mV) systems. In addition to peaks arising from CdTe at 161 cm^{-1}, peaks at 121 and 141 cm^{-1} can be identified as Te peaks. These elemental Te could appear as precipitates within the layer or Te thin film on the surface. As observed from PL (section 3.7) and the overall devices work (section 3.10), excess Te in the CdTe layers deteriorate its electronic properties.

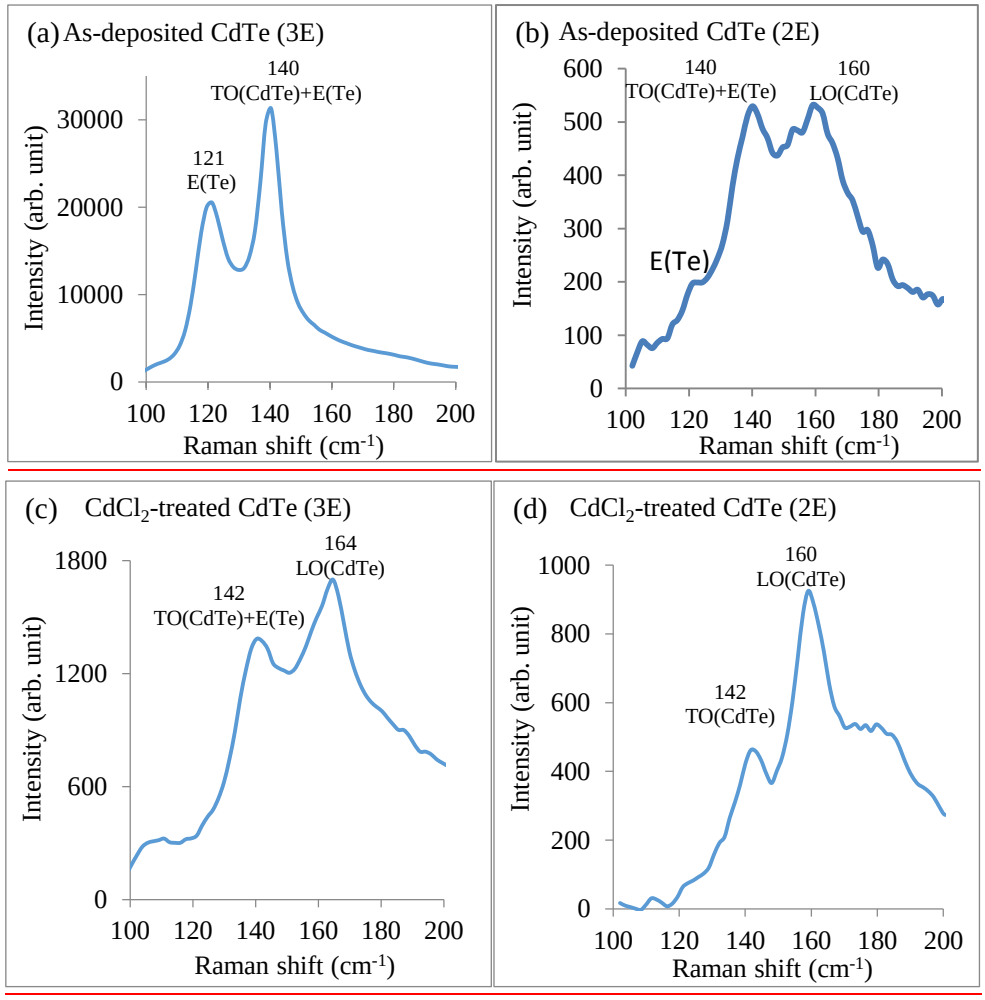

Figure 6. Plot of Raman spectra of CdTe thin films for as-deposited and $CdCl_2$-treated layers. The samples were grown using 3E (a & c) and 2E (b & d) respectively. The surfaces were thoroughly washed with deionised water after $CdCl_2$ treatment.

$CdCl_2$ treatment however, tend to reduce the elemental Te in the layers by reacting with Cd from $CdCl_2$ and forming CdTe, in addition to other benefits such as re-crystallisation, reduction of grain boundaries and defects, and doping. As shown in Figure 6, both CdTe layers from 3E and 2E systems show similar reduction of elemental Te from electroplated CdTe layers.

3.6. Optical absorption

Optical absorption studies were carried out in order to study the absorption edge and estimate the optical energy gap of the material. This analysis usually plot ($\alpha h\upsilon^2$) versus photon energy ($h\upsilon$) or Tauc plots to determine energy gap values. In this research programme, we have found that plots of square of optical absorption (A^2) versus photon energy ($h\upsilon$) also produce very similar results and therefore Figure 7 shows the plots obtained for electroplated CdTe layers using 3E and 2E systems.

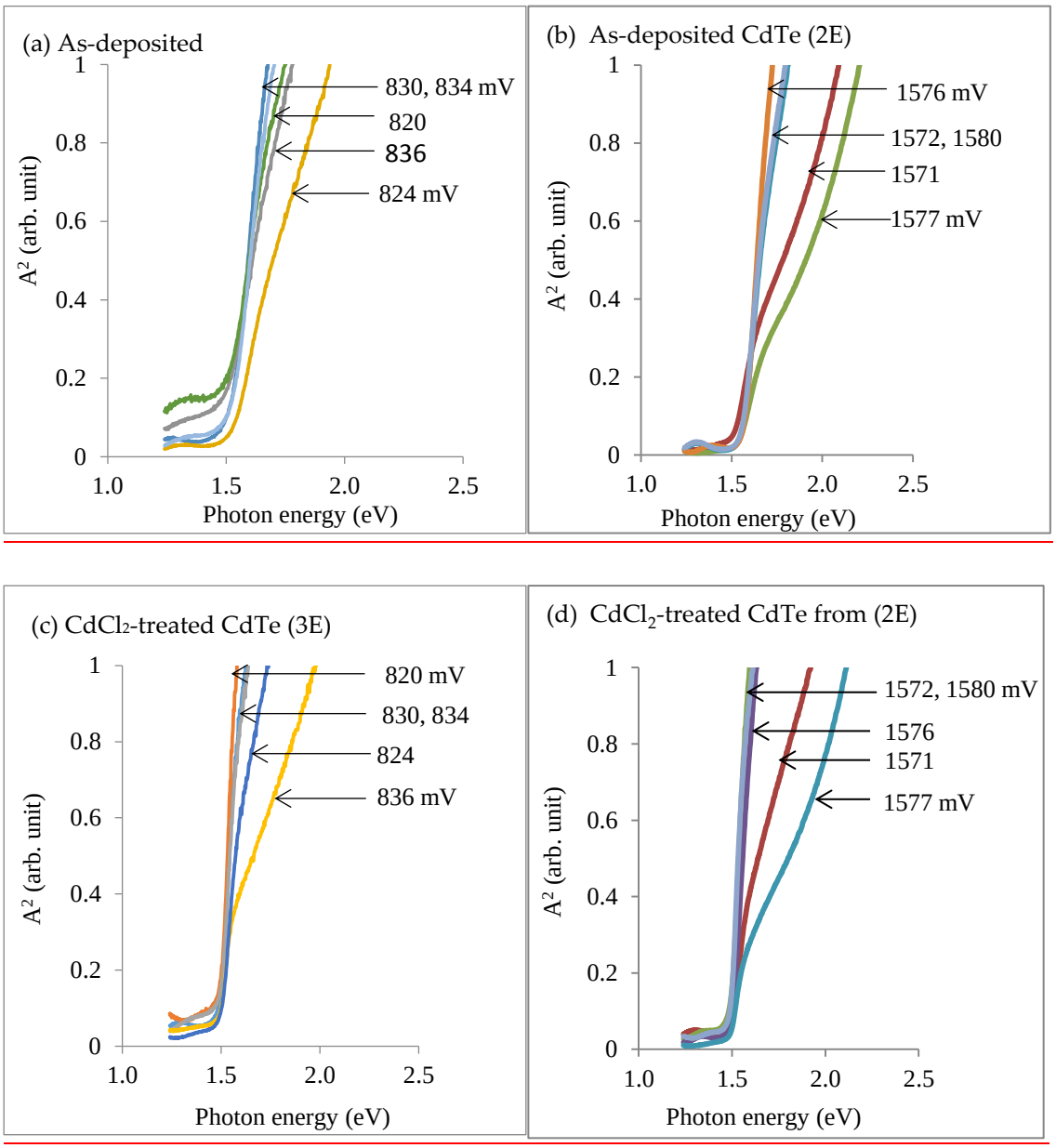

Figure 7. Optical absorption edges for as-deposited and $CdCl_2$-treated CdTe layers grown using 3E (a and c) and 2E (b and d) systems at different growth potentials. The films were heat-treated at 400°C for 15 minutes in air.

It is a notable feature of the curves that when the material layers are grown at PPS, the optical absorption edge is sharp and produces accurate E_g values. Stoichiometric CdTe layers grown using both 3E and 2E systems produce bandgap of 1.48 eV very close to that of bulk CdTe material. As the growth voltage deviates from the PPS, the slope of the absorption edge weakens, and produced E_g values away from the bulk energy gap. Presence of several phases in the layer tends to produce

smaller crystallites and hence produce slightly larger E_g values. Te precipitates, Te-rich CdTe and stoichiometric CdTe, when grown below PPS, are possible and the layer consists of smaller grains and more pinholes. More pinholes means passage of all wavelengths and therefore equivalent to lager bandgaps. Addition of more metallic cadmium when grown above PPS tends to reduce the bandgap due to metallic property of Cd.

3.7. Photoluminescence studies

Photoluminescence studies were carried out on both as-deposited and $CdCl_2$ treated CdTe layers obtained from 3E and 2E electrodeposition systems. The aim was to observe the defects structure in the materials' bandgap. The PL system used is capable of detecting materials' defects between 0.55 eV below the conduction band and the top of the valence band. Full details of the experimental set up and other PL work is published elsewhere [28].

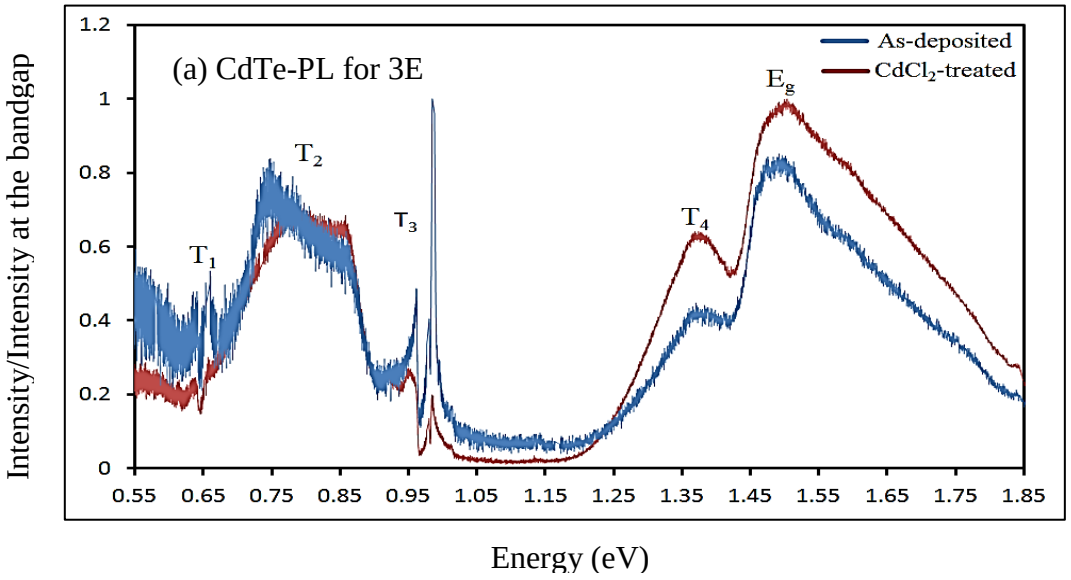

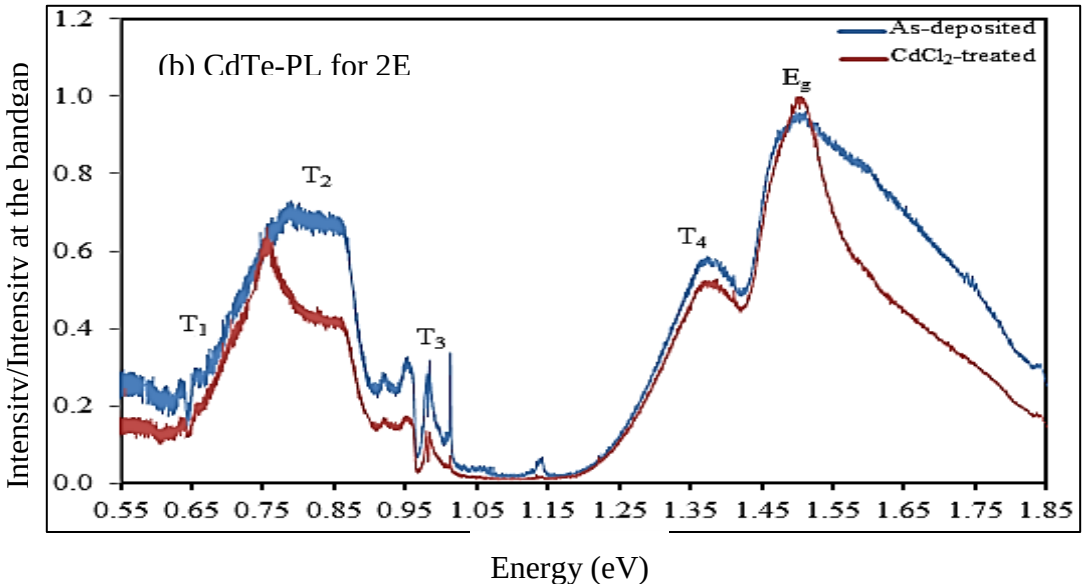

Figure 8. Photoluminescence spectra obtained for as-deposited and $CdCl_2$-treated CdTe layers grown from (a) 3E and (b) 2E systems.

Figure 8 shows the experimentally observed PL spectra for these CdTe layers for direct comparison. PL spectra from ED-CdTe layers grown from both 3E and 2E systems show similar defect structure. Defects finger-prints consist of four main defect distributions (T_1-T_4) and the near

band emission peak, labelled as E_g. The PL peaks are labeled as T_1-T_4, only to aid the discussion, but those broad peaks could include several peaks arising from closely situated defects. The summary of the emission levels are shown in Table 1 with approximate energy distributions.

Table 1. Summary of electron traps observed at 80 K for CdTe layers electroplated using 3E and 2E systems.

Energy (eV)	T_1±0.02 (eV)	T_2±0.15 (eV)	T_3±0.03 (eV)	T_4±0.08 (eV)	E_g peak (eV)
As-deposited (3E)	0.66	0.75	0.97	1.37	1.50
$CdCl_2$-treated (3E)	-	0.77	0.97	1.37	1.50
As-deposited (2E)	0.66	0.79	0.96	1.37	1.51
$CdCl_2$-treated (2E)	-	0.75	0.96	1.37	1.50

There are some important features to note in these PL spectra. The mid-gap peak labelled as T_2 is the most detrimental "Killer Centres" in CdTe and related to Te-richness in CdTe [29,30]. Therefore, these defects distribution must be related to tellurium antisites (Te_{Cd}), tellurium interstitials (Te_i) and cadmium vacancies (V_{Cd}). This defects distribution is very broad and spread over 0.30 eV, contributing to detrimental and effective recombination of photo-generated charge carriers. In the case of CdTe grown using 2E system, these defects reduction is more apparent after $CdCl_2$ treatment. Sharpening of the E_g peak is also clear for these layers. Therefore, based on the PL spectra, both materials are comparable, if not materials arising from 2E systems are slightly superior. In order to produce high efficiency devices, these mid-gap "Killer Centres" (T_2) should be completely removed, or at least minimised to reduce recombination of photo-generated charge carriers.

In the two references [29,30], it has been clearly demonstrated that the CdTe layers can be produced with Te-rich or Cd-rich conditions. This work also showed that largest Schottky barriers are produced on Cd-rich surfaces rather than Te-rich surfaces. Cd-rich CdTe removes mid-gap killer centres and pin the Fermi level close to the valence band maximum producing excellent diodes. Therefore high efficiency solar cells can be produced using Cd-rich CdTe layer as shown in Figure 9(b).

3.8. Ultraviolet Photoelectron Spectroscopy

In the development of thin film solar cells based on CdTe, the usual superstrate device structure used is glass/FTO/CdS/CdTe/back electrical contact. Since CdTe exists both in n-type and p-type conductivity, two PV devices are possible [31], as shown in Figure 9.

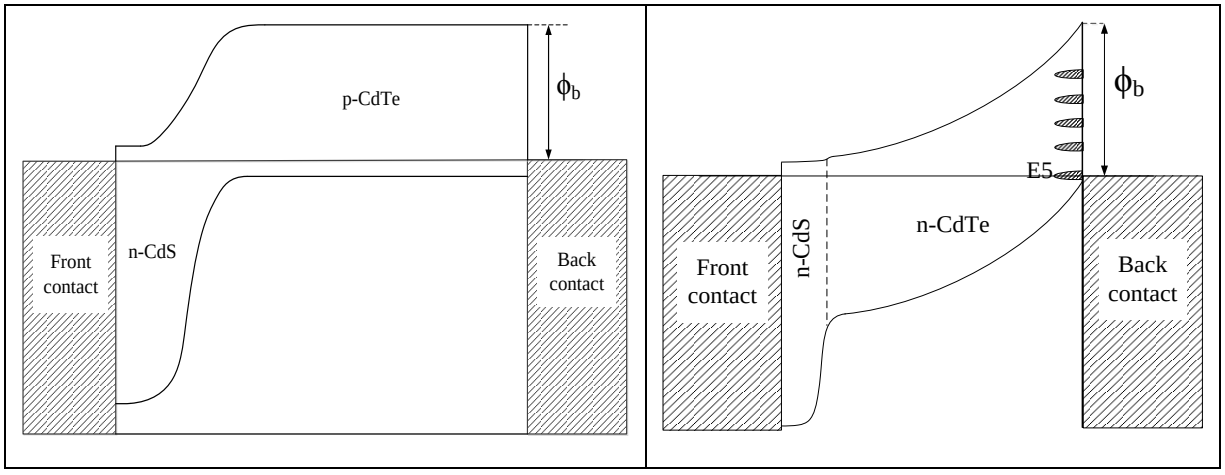

Figure 9. Possible device configurations when CdTe layers are used as (a) p-type and (b) n-type in electrical conduction.

The above structure forms a simple p-n junction when the CdTe layer is p-type, and forms an n-n heterojunction connected in parallel with a large Schottky barrier (SB) at the back metal contact (n-n+SB) when the CdTe layer is n-type. In both cases, the Fermi level (FL) should align very close to the valence band maximum, in order to produce high efficiency solar cells. However, strong FL pinning occurs at CdTe/metal interfaces as reported in reference [3]. Therefore, the knowledge on the positions of the FL at the CdTe back surface is useful in this device development program. In order to gather any useful information, ultraviolet photoelectron spectroscopy (UPS) studies were carried out. The detailed results on UPS and the observed results are published elsewhere [32].

After a comprehensive UPS study, it was found that the results need to be carefully analysed depending on the surface preparations. UPS is a surface sensitive technique (probing depth is one or two monolayers) and therefore results can depend on various factors such as length of exposure to the atmosphere. However, UPS results also provide valuable information on interactions at the CdTe/Au electrical contacts. It measures the work function of the Au layer deposited on CdTe, and that of CdTe surface. Typical values measured are shown in Table 2.

Table 2. Summary of work function measured for Au and CdTe surfaces using UPS.

Growth system	Material used	Work function of Au (eV)	Work function of CdTe (eV)
CdTe from 3E	CdTe ($CdCl_2$)	4.31	3.89
	CdTe ($CdSO_4$)	4.42	4.00
CdTe from 2E	CdTe ($CdSO_4$)	4.39	4.35
	CdTe ($Cd(NO_3)_2$)	4.60	3.61

The reported work functions for Au and Te are 5.10 eV [33] and 4.73 eV [34] respectively. It is clear that the average work function measured for Au contacts deposited on CdTe layer is ~ 4.40 eV, and less than 5.10 eV (see last column of Table 2). This confirms our previous conclusions based on soft-XPS results carried out at the synchrotron radiation laboratory in Daresbury. As Au is deposited on CdTe, a strong interaction takes place by Au alloying with Cd and releasing Te to the surface of the Au layer [3,35]. As a result, the Au layer is not pure Au, and consists of floating Te or Au_xTe_y alloy. Exposure to atmosphere could oxidise some of the Te into Te_xO_y as well. In fact, this can be visually observed in glass/FTO/CdS/CdTe/Au devices. As soon as the devices are made, the Au contacts show shiny Au colour. However, with time, the appearance of Au contacts show dull and Cu colour due to these microscopic interactions at the interface. This effect is shown on both Au/bulk CdTe, and Au/thin films of CdTe thin films grown using either 3E or 2E systems.

3.9. CdS/CdTe solar cells.

In this research programme, both 3E and 2E systems were used in parallel to electroplate CdTe from $CdSO_4$ precursor and to fabricate glass/FTO/CdS/CdTe/Au solar cells. Both materials are capable of producing PV active solar cells with varying conversion efficiencies in a wide range of ~(5-13)%. The efficiency depends from batch to batch and the cell parameters show wide variation.

This wide variations of efficiency is not unique to devices fabricated with electroplated CdTe layers. This seems to be a common feature for devices made by different growth techniques. Therefore, this should be an inherent property of poly-crystallite CdTe and need deep understanding of this material issue. Since the $CdCl_2$ treatment is a key processing step, full understanding is also essential to understand these efficiency variations. In addition, existence of pinholes, non-uniformity during growth, different defect concentrations at different points and varying doping concentrations could contribute to this large variation.

In this comprehensive research programme carried out over the past two decades, the growth was performed by more than six researchers using 3E system. However, the device efficiencies observed were variable and highest efficiency observed was 6.9%. Although the efforts devoted to CdTe growth using 2E system is less than half that of 3E system, the probability of achieving better performance is higher with 2E grown materials. Table 3 shows the parameters observed for the best solar cells to date using CdTe grown from 2E and 3E systems

Highest efficiency values observed to date for 2E is ~12.8% as shown in Figure 10 and Table 3. The I-V characteristics of dark and illuminated (AM 1.5) conditions for a device with CdTe grown by 2E system are shown in Figure 10. This structure also has a thin layer (~100 nm) of n-ZnS as a buffer layer, forming a 3-layer graded bandgap device. All possible device properties have been extracted from these I-V characteristics and summarised in Table 3. These excellent properties including very high short circuit current densities show the high potential of graded bandgap device structures [36,37]. These high efficiencies have been observed for CdTe materials grown using 2E systems. Although it is pre-mature to draw a firm conclusion, materials grown from 2E systems are comparable, if not superior to those grown from 3E system.

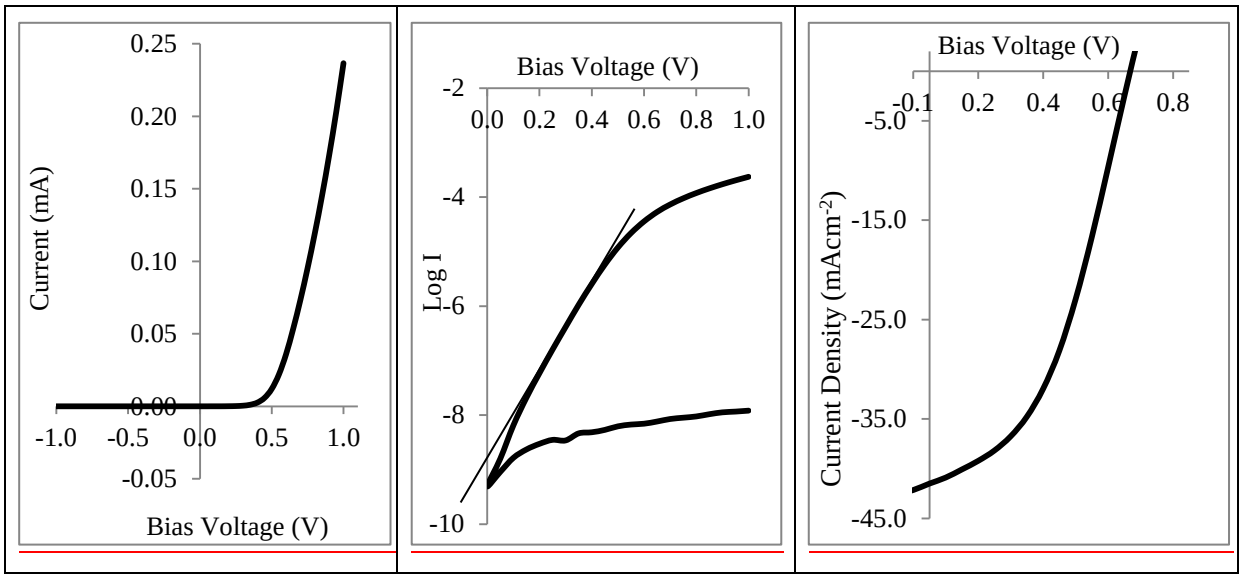

Figure 10. Typical I-V characteristics observed for glass/FTO/n-ZnS/n-CdS/n-CdTe/Au device with CdTe layers grown using 2E system.

Table 3. Summary of device parameters obtained from I-V characteristics for devices fabricated with CdTe grown by 2E and 3E systems.

I-V Parameters measured under dark condition						
Device parameter	RF	n	I_o (nA)	Φ_b (eV)	R_s (Ω)	R_{sh} (MΩ)
2E	$10^{4.3}$	1.88	~0.79	>0.81	~1351	→∞ (81)
3E	$10^{4.7}$	2.40	~1.00	>0.80	~277	→∞ (95)
I-V Parameters measured under AM 1.5 illumination						
Device parameter	V_{oc} (V)	J_{sc} (mAcm^{-2})	FF	η (%)	R_s (Ω)	R_{sh} (Ω)
2E	0.670	41.5	0.46	12.8	~134	~3819
3E	0.670	22.0	0.47	6.9	~185	~5270

4. Conclusions

The results presented in this paper leads to draw several conclusions.

1. Both 3E and 2E systems produce CdTe layers with similar structural properties. CdTe material is poly-crystalline, with cubic crystal structure and grow with (111) preferential orientation. The only difference observed is the higher growth rate when 2E system is used and this is an added advantage in a production line.

2. Morphologies of the CdTe layers are very similar. In as-deposited layers, FTO substrate is covered by large CdTe agglomerations, consisting of small crystallites. The sizes of the crystallites vary from 20-65 nm, as estimated by XRD measurements. Upon $CdCl_2$ treatment, these crystallites merge into large crystals ranging into few microns size. Then, the layers are comparable with materials grown by high temperature techniques such as the closed space sublimation. IPL treatment provides a convenient rapid thermal annealing method suitable for flexible substrates and role-to-role production methods. SEM images also indicate the melting of grain boundary regions during heat-treatment in the presence of $CdCl_2$.

3. CdTe layers grown from both methods seem to have elemental Te as precipitates or a surface layer. $CdCl_2$ treatment removes these excessive Te, and makes the material more stoichiometric. Comprehensive device work also shows that Te-richness is detrimental for devices, and stoichiometric or Cd-rich CdTe is more suitable for enhanced device performance.

4. Both 3E and 2E systems allow the growth of p- and n-type CdTe layers. Te-richness produce p-type material and Cd-richness produce n-type CdTe. Both methods produce high crystallinity at the Perfect Point of Stoichiometry (PPS) and the energy bandgap measured for stoichiometric material is close to the bandgap of bulk CdTe (~1.45 eV).

5. PL spectra of CdTe layers grown from 3E and 2E systems have similar finger-prints. $CdCl_2$ treatment shows the reduction of some defects, and the materials arising from 2E system show improved quality in terms of defect concentrations.

6. UPS results summarised and soft-XPS results reported before show a strong intermixing at the CdTe/Au interface. This may lead to degradation of devices and therefore a reaction barrier should be introduced in order to improve the stability and lifetime of the devices.

7. From a large number of devices fabrication experience, both CdTe layers grown by 3E and 2E systems show wide variation of efficiency values between ~5-13%. Although premature to draw firm conclusions, highest efficiency values observed to date in our research laboratories have been fabricated using CdTe layers grown by 2E system. Therefore, elimination of a possible impurity source (reference electrode) introduces several advantages such as improving the growth rate, system simplification, cost reduction and ability to grow improved materials at elevated temperatures and hence fabrication of comparable or better performing devices.

Acknowledgement: Authors would like to thank A.P. Samantilleke, Nandu Chaure, G. Muftah, Jayne Wellings, N. A. Abdul-Manaf, A.A. Ojo and H.I. Salim for their contributions to this work.

Author Contributions: SHU-Solar Energy Group members (I.M. Dharmadasa, M.L. Madugu and O.I. Olusola): conceived, designed, writing of the paper, Electrodeposition of CdS and CdTe, materials characterisation, device fabrication and assessment, interpretation of results, understanding the science behind materials and devices, drafting of manuscript, drawing diagrams and completing the paper. O. K. Echendu, F. Fauzi, D. G. Diso, A.R. Weerasinghe: Development of materials and optimisation.Conn Center for Renewable Energy Research, University of Louisville, Louisville, Kentucky 40292, USA Group members (T. Druffel, R. Dharmadasa, B. Lavery J.B. Jasinski, T.A. Krentsel, and G. Sumanasekera): Carried out Photoluminescence (PL) experiment and analysis.

Conflicts of Interest: The authors declare no conflicts of interest.

References

1. B.M. Basol, High-efficiency electroplated heterojunction solar cell, *J. Appl. Phys.*, **55** (1984) 601–603. doi:10.1063/1.333073.
2. Y.P. Gnatenko, P.M. Bukivskij, S. Opanasyuk, D.I. Kurbatov, M.M. Kolesnyk, V. V. Kosyak, H. Khlyap, Low-temperature photoluminescence of II-VI films obtained by close-spaced vacuum sublimation, *J. Lumin.*, **132** (2012) 2885–2888. doi:10.1016/j.jlumin.2012.06.003.
3. I.M. Dharmadasa, Recent developments and progress on electrical contacts to CdTe, CdS and ZnSe with special reference to barrier contacts to CdTe, *Prog. Cryst. Growth Charact. Mater.*, **36** (1998) 249–290. doi:10.1016/S0960-8974(98)00010-2.
4. R.H. Bube, Photovoltaic Materials, 1st ed.; R.C. Newman; Imperial College Press: London, UK, 1998; Vol. 1 pp 6, 1st ed., n.d.
5. M. Takahashi, K. Uosaki, H. Kita, Y. Suzuki, Effects of heat treatment on the composition and semiconductivity of electrochemically deposited CdTe films, *J. Appl. Phys.*, **58** (1985) 4292. doi:10.1063/1.335514.
6. N.B. Chaure, a. P. Samantilleke, I.M. Dharmadasa, The effects of inclusion of iodine in CdTe thin films on material properties and solar cell performance, *Sol. Energy Mater. Sol. Cells.*, **77** (2003) 303–317. doi:10.1016/S0927-0248(02)00351-3.
7. I.M. Dharmadasa, P.A. Bingham, O.K. Echendu, H.I. Salim, T. Druffel, R. Dharmadasa, G.U. Sumanasekera, R.R. Dharmasena, M.B. Dergacheva, K.A. Mit, K.A. Urazov, L. Bowen, M. Walls, A. Abbas, Fabrication of CdS/CdTe-Based Thin Film Solar Cells Using an Electrochemical Technique, *Coatings.*, **4** (2014) 380–415. doi:10.3390/coatings4030380.
8. M.G. Panthani, J.M. Kurley, R.W. Crisp, T.C. Dietz, T. Ezzyat, J.M. Luther, D. V. Talapin, High Efficiency Solution Processed Sintered CdTe Nanocrystal Solar Cells: The Role of Interfaces, *Nano Lett.*, **14** (2014) 670–675. doi:10.1021/nl403912w.
9. K. Sugiyama, Properties of CdTe films grown on InSb by molecular beam epitaxy, *Thin Solid Films.*, **115** (1984) 97–107. doi:10.1016/0040-6090(84)90511-X.
10. I. Mora-Seró, R. Tena-Zaera, J. González, V. Muñoz-Sanjosé, MOCVD growth of CdTe on glass: analysis of in situ post-growth annealing, *J. Cryst. Growth.*, **262** (2004) 19–27. doi:10.1016/j.jcrysgro.2003.10.033.
11. B. Ghosh, S. Hussain, D. Ghosh, R. Bhar, a. K. Pal, Studies on CdTe films deposited by pulsed laser deposition technique, *Phys. B Condens. Matter.*, **407** (2012) 4214–4220. doi:10.1016/j.physb.2012.07.006.
12. M.P.R. Panicker, Cathodic Deposition of CdTe from Aqueous Electrolytes, *J. Electrochem. Soc.*, **125** (1978) 566. doi:10.1149/1.2131499.
13. R.K. Pandey, S.B. Sahu, S. Chandra, Handbook of semiconductor electrodepotion, Marcel Dekker, Inc, New York, 1996.
14. N. Abdul-Manaf, H. Salim, M. Madugu, O. Olusola, I. Dharmadasa, Electro-Plating and Characterisation of CdTe Thin Films Using CdCl2 as the Cadmium Source, *Energies.*, **8** (2015) 10883–10903. doi:10.3390/en81010883.
15. K. Arai, J. Kawaguchi, K. Murase, T. Hirato, Y. Awakura, Effect of Chloride Ions on the Electrodeposition Behavior of CdTe from Ammoniacal Basic Electrolytes, *J. Surf. Finish. Soc. Japan.*, **57** (2006) 70–76. doi:10.4139/sfj.57.70.
16. R.N. Bhattacharya, K. Rajeshwar, Heterojunction CdS/CdTe solar cells based on electrodeposited p-CdTe thin films: Fabrication and characterization, *J. Appl. Phys.*, **58** (1985) 3590. doi:10.1063/1.335735.
17. D. Lincot, Electrodeposition of semiconductors, *Thin Solid Films.*, **487** (2005) 40–48. doi:10.1016/j.tsf.2005.01.032.
18. D. Cunningham, M. Rubcich, D. Skinner, Cadmium telluride PV module manufacturing at BP Solar, *Prog. Photovoltaics Res. Appl.*, **10** (2002) 159–168. doi:10.1002/pip.417.
19. H.I. Salim, V. Patel, A. Abbas, J.M. Walls, I.M. Dharmadasa, Electrodeposition of CdTe thin films using nitrate precursor for applications in solar cells, *J. Mater. Sci. Mater. Electron.*, **26** (2015) 3119–3128. doi:10.1007/s10854-015-2805-x.
20. First Solar's Cells Break Efficiency Record, https://www.technologyreview.com/s/600922/first-solars-cells-break-efficiency-record, consulted May, (2016).

21. S. Dennison, Dopant and Impurity Effects in Electrodeposited CdS/CdTe Thin Films for Photovoltaic Applications, *J. Mater. Chem.*, **4** (1994) 41–46.
22. O.K. Echendu, K. Okeoma, C.I. Oriaku, I.M. Dharmadasa, Electrochemical Deposition of CdTe Semiconductor Thin Films for Solar Cell Application Using Two-Electrode and Three-Electrode Configurations: A Comparative Study, accepted for publication in, *Adv. Mater. Sci. Eng.*, (2016).
23. R. Dharmadasa, B.W. Lavery, I.M. Dharmadasa, T. Druffel, Processing of CdTe thin films by intense pulsed light in the presence of CdCl 2, *J. Coatings Technol. Res.*, **12** (2015) 835–842. doi:10.1007/s11998-015-9688-x.
24. D.G. Diso, Research and development of CdTe based thin film PV solar cells, PhD Thesis, Sheffield Hallam University, (2011). http://shura.shu.ac.uk/4941/.
25. I.M. Dharmadasa, O.K. Ehendu, F. Fauzi, N.A. Abdul-Manaf, O.I. Olusola, H.I. Salim, M.L. Madugu, A.A. Ojo, Improvement of composition of CdTe thin films during heat treatment in the presence of CdCl2, *Coatings, Submitt. Process.*, (2016).
26. J.T. Cheung, Role of atomic tellurium in the growth kinetics of CdTe (111) homoepitaxy, *Appl. Phys. Lett.*, **51** (1987) 1940–1942. doi:10.1063/1.98307.
27. P. Fernandez, Defect Structure and Luminescence Properties of CdTe Based Compounds, *J. Optoelectron. Adv. Mater.*, **5** (2003) 369–388.
28. I.M. Dharmadasa, O.K. Echendu, F. Fauzi, N.A. Abdul-Manaf, H.I. Salim, T. Druffel, R. Dharmadasa, B. Lavery, Effects of CdCl2 treatment on deep levels in CdTe and their implications on thin film solar cells: a comprehensive photoluminescence study, *J. Mater. Sci. Mater. Electron.*, **26** (2015) 4571–4583. doi:10.1007/s10854-015-3090-4.
29. I.M. Dharmadasa, J.M. Thornton, R.H. Williams, Effects of surface treatments on Schottky barrier formation at metal/n-type CdTe contacts, *Appl. Phys. Lett.*, **54** (1989) 137. doi:10.1063/1.101208.
30. Z. Sobiesierski, I.M. Dharmadasa, R.H. Williams, I.M. Dharmadasa, R.H. Williams, Correlation of photoluminescence measurements with the composition and electronic properties of chemically etched CdTe surfaces, **2623** (1990). doi:10.1063/1.100178.
31. I.M. Dharmadasa, Advances in Thin-Films Solar Cells, 1st ed., Pan Stanford Publishing Pte. Ltd,: Singapore, 2012.
32. I.M. Dharmadasa, O.K. Echendu, F. Fauzi, H.I. Salim, N.A. Abdul-Manaf, J.B. Jasinski, A. Sherehiy, G. Sumanasekera, Study of Fermi level position before and after CdCl2 treatment of CdTe thin films using ultraviolet photoelectron spectroscopy, *J. Mater. Sci. Mater. Electron.*, (2016). doi:10.1007/s10854-016-4391-y.
33. CRC Handbook of Chemistry and Physics, CRC Press, Cleveland, Ohio, 1977.
34. K. Okuyama, J. Tsuhako, Y. Kumagai, Behavior of Metal Contacts to Evaporated Tellurium Films, *Thin Solid Films*., **30** (1975) 119–126.
35. N.M. Forsyth, I.M. Dharmadasa, Z. Sobiesierski, An investigation of metal contacts to II–VI compounds: CdTe and CdS, *Vacuum*., **38** (1988) 369–371. doi:10.1016/0042-207X(88)90081-4.
36. I.M. Dharmadasa, A. Ojo, H. Salim, R. Dharmadasa, Next Generation Solar Cells Based on Graded Bandgap Device Structures Utilising Rod-Type Nano-Materials, *Energies*., **8** (2015) 5440–5458. doi:10.3390/en8065440.
37. O. Echendu, I. M. Dharmadasa, Graded-Bandgap Solar Cells Using All-Electrodeposited ZnS, CdS and CdTe Thin-Films, *Energies*., **8** (2015) 4416–4435. doi:10.3390/en8054416.